Molecular Biology of the Cell
Vol. 9, 3195–3209, November 1998

Morphogenetic Effects of Neuregulin (Neu Differentiation Factor) in Cultured Epithelial Cells

Alexander Chausovsky,* Ilan Tsarfaty,† Zvi Kam,* Yosef Yarden,‡ Benjamin Geiger,* and Alexander D. Bershadsky*§

Departments of *Molecular Cell Biology and ‡Biological Regulation, The Weizmann Institute of Science, Rehovot 76100, Israel; and †Department of Human Microbiology, Sackler School of Medicine, Tel Aviv University, Tel Aviv 69978, Israel

Submitted May 1, 1998; Accepted August 28, 1998
Monitoring Editor: Tony Hunter

Neuregulin, or neu differentiation factor, induces cell proliferation or differentiation through interaction with members of the ErbB family of receptor tyrosine kinases. We report that neuregulin can also induce profound morphogenic responses in cultured epithelial cells of different origins. These effects include scattering of small epithelial islands and rearrangement of larger cell islands into ordered ring-shaped arrays with internal lumens. The ring-forming cells are interconnected by cadherin- and β-catenin-containing adherens junctions. In confluent cultures, neuregulin treatment induces formation of circular lumenlike gaps in the monolayer. Both cell scattering and ring formation are accompanied by a marked increase in cell motility that is independent of hepatocyte growth factor/scatter factor and its receptor (c-Met). Affinity-labeling experiments implied that a combination of ErbB-2 with ErbB-3 mediates the morphogenic signal of neuregulin in gastric cells. Indeed, a similar morphogenic effect could be reconstituted in nonresponsive cells by coexpression of ErbB-2 and -3. We conclude that a heterodimer between the kinase-defective neuregulin receptor, ErbB-3, and the coreceptor, ErbB-2, mediates the morphogenetic action of neuregulin.

INTRODUCTION

A variety of developmental processes, including embryonic development and tissue morphogenesis, depend on structural reorganization of individual cells and cell groups. Alterations in cell morphology, in turn, are driven by coordinated changes in cell motility, adhesion, and cytoskeletal organization (Trinkaus, 1984; Bray, 1992). Morphogenetic processes are of a particular importance in epithelial cells, which form coherent layers that expand, contract, and often fold into tubular or alveolar structures (Bray, 1992). Epithelial tissue can also disintegrate into separate motile cells in a process known as epithelial–mesenchymal transition (Savagner *et al.*, 1994; Birchmeier and Birchmeier, 1995; Hay, 1995). All these processes are controlled by specific morphogenetic genes and depend both on specific developmental programs and external signals triggered by the extracellular matrix (ECM) and soluble ligands (growth factors). With the aid of these ligands, the behavior of epithelial cells can be controlled by the surrounding mesenchyme.

A well-studied system in which epithelial cells display ligand-dependent morphogenic behavior is based on hepatocyte growth factor/scatter factor (HGF/SF) and its receptor c-Met (Stoker *et al.*, 1987; Gherardi *et al.*, 1993). The scattering effect of HGF/SF depends on the activation of c-Met tyrosine kinase (Bottaro *et al.*, 1991; Naldini *et al.*, 1991), which in turn phosphorylates a number of downstream targets (Sachs *et al.*, 1996; Weidner *et al.*, 1996; Tamagnone and Comoglio, 1997). Besides cell scattering, under special culture conditions, HGF/SF treatment induces formation of branching, multicellular tubular structures (Montesano *et al.*, 1991; Soriano *et al.*, 1995; Yang *et al.*, 1995), suggesting that HGF/SF and c-Met may induce the formation of glandular structures in vivo (Tsarfaty *et al.*, 1992; Tsarfaty *et al.*, 1994). However, it was

§ Corresponding author. E-mail address: libersha@weizmann.weizmann.ac.il.

recently shown that epidermal growth factor (EGF) can replace HGF/SF in kidney tubule formation in *met* knockout mice (Kjelsberg *et al.*, 1997).

The HGF/SF and c-Met signaling is not the only inducer of cell scattering in monolayer cultures. Acidic fibroblast growth factor, for example, can efficiently induce epithelial–mesenchymal transition and cell scattering in some types of epithelial cells (Boyer *et al.*, 1993; Savagner *et al.*, 1994; Savagner *et al.*, 1997). Among the growth factor receptors involved in cell scattering are c-ros, c-neu (ErbB-2), keratinocyte growth factor receptor, and trk A. On the other hand, only c-Met activation was reported to induce the more complex set of morphogenetic changes, including the formation of the branching tubules in three-dimensional collagen gel (Sachs *et al.*, 1996).

In the present work we studied the morphogenetic effects of neuregulin, also known as neu differentiation factor (NDF) or heregulin. Receptors to neuregulins belong to the ErbB family of receptor protein kinases and are widely expressed in many cell types of different organisms from *Caenorhabditis elegans* to humans (Burden and Yarden, 1997). In mammals the neuregulin–ErbB signaling networks were shown to be involved in many systems, including cardiac development, Schwann cell and oligodendrocyte differentiation, and some aspects of neuronal development, as well as in the formation of neuromuscular synapses (Burden and Yarden, 1997). The involvement of neuregulin–ErbB signaling in epithelial morphogenesis is especially interesting. With the exception of ErbB-4, whose expression is limited to certain epithelia, the other three ErbB family receptors are widely present in epithelial cells, whereas mesenchymal cells usually express high levels of the neuregulin family ligands (Burden and Yarden, 1997). These data suggest that neuregulin–ErbB signaling might be involved in epithelial–mesenchymal interaction. In fact, recent studies suggest that neuregulin signaling participates in mammary gland development, where it probably works in concert with HGF/SF (Yang *et al.*, 1995; Jones *et al.*, 1996). These studies were based mainly on the analysis of neuregulin effects in organ cultures of mammary glands.

In the present work we show that neuregulin can induce various types of morphogenetic responses, ranging from complete scattering to the formation of unique multicellular ring-shaped structures even in monolayer cultures of epithelial cells. Neuregulin was shown to be a potent motogen for cultured epithelial cells, whereas the majority of cell–cell adherens junctions were not disrupted upon neuregulin treatment. We have further demonstrated that these motogenic and morphogenic effects are specific to neuregulin and do not involve the activation of the c-Met signaling pathway. We also show that activation of the ErbB-2 and -3 receptor heterodimers is responsible for this neuregulin-induced epithelial morphogenesis.

MATERIALS AND METHODS

Cell Culture and Ligand Treatment

Human gastric carcinoma cell line N87 (Park *et al.*, 1990) was obtained from Dr. A. Gazdar (National Cancer Institute, Bethesda, MD). We also used a subline of a human breast carcinoma cell line, T47D, which expresses low levels of c-Met receptor (Keydar *et al.*, 1979). The CB-1, CB-2, CB-3, and CB-4 cell lines are Chinese hamster ovary (CHO) cells stably overexpressing ErbB-1, -2, -3, and -4, respectively (Tzahar *et al.*, 1996). In some experiments we also used squamous carcinoma cell line A431, breast carcinoma cell line MCF 7, prostate carcinoma cell line DU 145 (Stone *et. al.*, 1978), and ovarian cell carcinoma cell line IGROV-1 (Ma *et. al.*, 1998). These cell lines were kindly provided to us by Dr. Z. Eshhar (Department of Immunology, The Weizmann Institute of Science, Rehovot, Israel). The cultures were routinely cultivated in Dulbecco's modified Eagle's medium (DMEM), supplemented with 10% bovine calf serum (Hyclone, Logan, UT) in a humidified atmosphere with 7.5% CO_2 at 37°C. For the microscopic observation of living cells, the cultures in L15 (Leibovitz) medium, with or without added ligands, were used. A trypsin and EDTA mixture was used for subculturing.

In the first type of experiments, 5×10^4 cells were plated on 18×18-mm^2 coverslips, cultured overnight in serum-containing medium, washed once with serum-free medium, and incubated for an additional 1–2 h. These serum-starved cells were then used in the scattering experiments. Alternatively, when the effect of ligands on the mature colonies was studied, 5×10^3 cells per coverslip were plated in serum-containing medium, and the cells were maintained for 4–7 d. Then the ligand was added into serum-free DMEM for different time intervals. To study the effects of ligands on confluent monolayers, a dense cell suspension (10^6 cells/ml) was plated overnight in a 300-μl drop of serum-containing medium, and the ligand was added to the monolayers for 4–7 d thereafter.

Recombinant rat or human neuregulin ligands, produced in CHO cells, were obtained from Amgen (Thousand Oaks, CA). CHO-rat NDF-β4 was used in the majority of the experiments. NDF-α1 and -α2, EGF-like domain of NDF-β1 (ED NDF-β1), heparin-binding EGF, transforming growth factor-α (all from Amgen), and EGF (catalog number E-1257; Sigma Israel Chemicals, Rehovot, Israel) were also used in some experiments. HGF/SF was purified from NIH 3T3 cells transfected with *HGF/SF* as previously described (Rong *et al.*, 1993). The effect of ligands was analyzed in the concentration range of 1–100 ng/ml.

Immunoprecipitation and Western Blotting

Cells cultured on 50-mm Falcon dishes (Falcon, Lincoln Park, NJ) or on coverslips were washed with PBS and dissolved in 1 ml lysis buffer containing 50 mM HEPES (pH 7.5), 150 mM NaCl, 1% Triton X-100, 10% glycerol, 1.5 mM $MgCl_2$, 1 mM Na-orthovanadate, 180 μg/ml aprotinin, 2 mM PMSF, and 180 μg/ml leupeptin. Insoluble material was removed by centrifugation. Protein A Sepharose (CL-4B; Pharmacia, Uppsula, Sweden) or anti-mouse immunoglobulin G agarose beads (Sigma) were suspended in immunoprecipitation buffer (20 mM HEPES, 150 mM NaCl, 0.1% Triton X-100, 10% glycerol, pH 7.5) and incubated with the primary antibodies. After washing with the immunoprecipitation buffer, the beads were incubated with the cell lysates (containing equal amounts of total cell proteins as determined by the Bradford method) for 90 min at 4°C. Immunoprecipitated proteins were extracted by boiling the washed beads in electrophoresis sample buffer and examined by gradient (5–15%) SDS-PAGE. For Western blot analysis, electrophoretic bands were electroblotted onto nitrocellulose membranes (Hybond-C; Amersham, Buckinghamshire, United Kingdom) and probed with the various primary antibodies, followed by horserad-

ish peroxidase–labeled secondary anti-mouse antibodies or protein A (Amersham). The list of primary antibodies used included rabbit polyclonal antibodies to NDF (Amgen), ErbB-1–4 (Santa Cruz Biotechnology, Santa Cruz, CA), and HGF/SF (Koochekpour *et al.*, 1997) and mouse monoclonal antibodies to ErbB-1–4 (Chen *et al.*, 1996). Immunoreactive bands were detected by enhanced chemiluminescence, using reagents from Kirkegaard and Perry (Gaithersburg, MD) and RX films from Fuji Photo Film (Tokyo, Japan).

Radiolabeling of Ligands, Covalent Cross-Linking, and Ligand Binding Assays

Soluble ligands (5 μg of CHO-rat NDF-β4 or ED NDF-β1) were mixed in an Iodogen-coated (Pierce Chemical, Rockford, IL) tube with $Na^{125}I$ (1 mCi). After 15 min incubation at 23°C, the mixture was separated on an Excellulose GF-5 column (Pierce). The specific activity of ^{125}I-labeled ligands ranged between 2×10^5 and 5×10^5 cpm/ng. For ligand binding 1–2×10^5 cells in 24-well dishes (Nunclone; Nunc, Roskilde, Denmark) were washed once with DMEM, supplemented with 0.1% BSA (binding buffer), and incubated for 2 h at 4°C with different concentrations of ^{125}I-labeled ligand. After three washes with binding buffer, cells were lysed for 15 min at 37°C with 0.5 ml of 0.1 N NaOH containing 0.1% SDS, and the radioactivity was determined using a γ counter. Specific binding was calculated by subtracting the binding of radiolabeled ligands to cells in the presence of a 100-fold excess of unlabeled ligand.

For covalent cross-linking analysis, 10^7 cells in six-well dishes were incubated on ice for 2 h with 10 ng/ml iodinated soluble ligand. The chemical cross-linking reagent disuccinimidyl suberate (Pierce) was added (1 nM) for 45 min on ice. The cells were then washed with PBS, lysed, and analyzed by gel electrophoresis.

Microscopy

For observation of living cells, the coverslips were mounted in the microscope chamber at 37°C in L15 serum-free medium. Photographs were taken at different time points before and after addition of the ligand, using Nomarsky (differential interference contrast) optics in a Zeiss (Thornwood, NJ) Axiophot microscope with a water immersion 40×, 0.75 numerical aperture (NA) Achroplan objective or using phase-contrast optics in Zeiss Axiovert with a 16×, 0.4 NA Neofluar objective. The images were acquired using a charge-coupled device camera (Photometrics, Tucson, AZ) and enhanced by Priism (Applied Precision, Issaquah, WA) software with a Silicon Graphics (Mountain View, CA) workstation.

For fluorescence staining, the cells on coverslips were simultaneously fixed and permeabilized in 3% paraformaldehyde and 0.5% Triton X-100 in PBS for 2 min, and postfixed in 3% paraformaldehyde for 20 min. The following primary antibodies were used: rabbit anti-pan cadherin (C3678; Sigma), rabbit anti-β-catenin (C2206; Sigma), monoclonal anti-plakoglobin (11E4) kindly provided by Dr. M.J. Wheelock (University of Toledo, Toledo, OH), and a monoclonal antibody to desmoglein kindly provided by Dr. W.W. Franke (German Cancer Research Center, Heidelberg, Germany). FITC- and TRITC-labeled goat antibodies to mouse and rabbit immunoglobulins (Jackson ImmunoRearch, West Grove, PA) were used as secondary antibodies. Actin was stained with FITC- or TRITC-labeled phalloidin (Sigma). Stained cultures were examined with an Axiophot microscope equipped with a 100×, 1.3 NA Plan-Apochromat objective and photographed using Tmax 3200 film (Eastman Kodak, Rochester, NY). Stained cells were also analyzed using a Zeiss confocal laser scanning microscope (LSM 410) equipped with a 25-mW krypton-argon laser and a 10-mW HeNe laser (488, 543, and 633 maximum lines), as previously described (Tsarfaty *et al.*, 1992).

Cell Motility and Scattering Measurements

To assess the rate of cell motility, the phagokinetic track method was used (Albrecht-Buehler, 1977). Eighteen-millimeter coverslips were coated with colloidal gold, and 2×10^3 cells were seeded on each coverslip. Medium was changed to a serum-free medium 4 h thereafter with or without β4-neuregulin (10 ng/ml), and incubation proceeded overnight (20 h). The cells were fixed as described above, stained with DAPI to visualize nuclei, and examined by fluorescence and dark-field microscopy using a 10× Plan-Neofluar objective. The areas of tracks were determined by projecting individual tracks on a screen and measuring 40–50 randomly selected tracks for each treatment.

The degree of cell scattering was estimated using an index of aggregation commonly used in ecological studies (Pielou, 1969). For this, the number of cells per field in control and treated cultures was counted after DAPI staining using a 100× Plan-Apochromat objective. Fifty independent fields were scored, and the variance (V) and mean (M) of cell numbers per field were calculated. The index of aggregation (I_A) value is defined as $I_A = V/M$. This index is equal to 1 when the distribution of the cells is random, and the higher this value, the more "patchy" the cell distribution is (Pielou, 1969).

RESULTS

Neuregulin Induces Scattering and Formation of Ring-Shaped Multicellular Structures in Epithelial Cell Cultures

To study the effects of neuregulin, N87 human carcinoma cells were plated at three different densities. Plating of 150 cells per 1 mm^2 followed by 1 d of incubation in 10% serum-containing medium resulted in the formation of small cell aggregates consisting of 5–10 cells (Figure 1A). After 1 h of serum starvation, neuregulin was added in serum-free DMEM for 24 h. Examination of the cells by phase-contrast microscopy or DAPI staining indicated that this treatment induced scattering (Figure 1, B and C). Quantitative analysis of scattering (see MATERIALS AND METHODS) shows that treatment with the β4 isoform of neuregulin (NDF-β4, 10 ng/ml) reduced the index of aggregation in N87 cells from 4.2 in control culture to 1.7. Other isoforms of neuregulin (NDF-α1 and -α2) induced a similar effect. In contrast, neither the addition of 10% serum nor treatment with EGF, heparin-binding EGF, or transforming growth factor-α induced a significant decrease in the degree of cell aggregation (our unpublished results).

In a second set of experiments, cells were plated at a very high density, resulting in the formation of a confluent monolayer within 4 h (Figure 1G). Treatment of the cells with NDF-β4 (100 ng/ml) for up to 5 d in serum-free medium induced formation of lumen-like cavities in the monolayer (Figure 1, H and I).

The most intriguing morphogenic effect was observed when cells were plated on the coverslips at a low density (15 cells/mm^2) and cultured for 3–4 d in normal medium until coherent colonies containing 10–50 cells were formed (Figure 1D). When stimulated with neuregulin for an additional period of up to 3 d in serum-free medium, these colonies transformed into multicellular rings (Figure 1F), whereas untreated colonies did not change (Figure 1E). The size of these rings was proportional to the cell number in the orig-

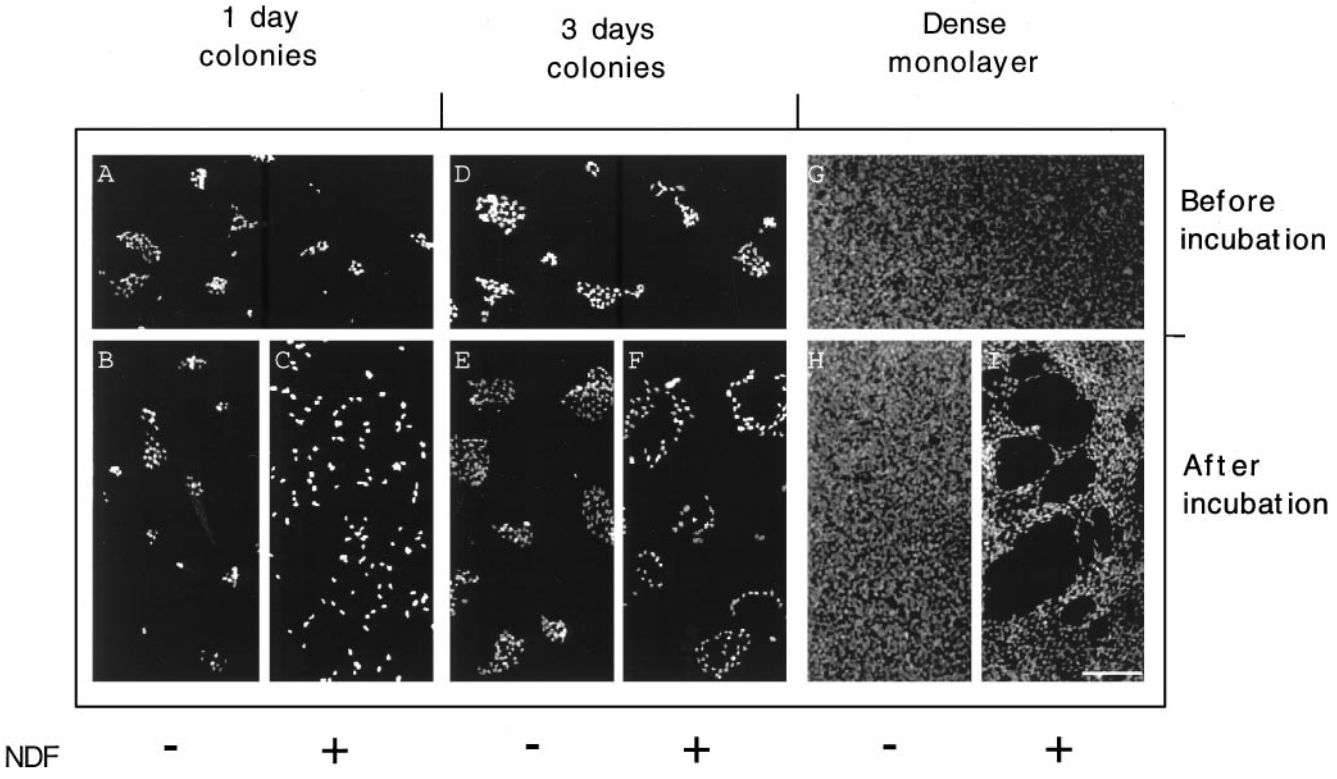

Figure 1. Effect of neuregulin on N87 cell distribution in cultures of different ages and densities. (A, D, and G) Cultures before neuregulin treatment. (B, C, E, F, H, and I) Cells after incubation in serum-free DMEM with (C, F, and I) and without (B, E, and H) NDF-β4. The concentration of NDF-β4 was 10 ng/ml (C) and 100 ng/ml (F and I). Cells were stained with DAPI. The culture conditions were as described in MATERIALS AND METHODS. Note complete scattering of small colonies in C, formation of ring-shaped structures in F, and lumenlike cavities in I. Bar, 100 μm.

inal colony. When relatively few cells were present in the original colony, a single-row ring was formed (Figure 1F), whereas relatively large colonies transformed into multirow rings (Figure 2, A and C).

To determine whether the formation of cell-free areas in the central part of the annular structure is due to cell death in the central part of the colony, we followed the process by DAPI staining, which can reveal apoptotic nuclei. Examination of the cells at different time points did not provide evidence for apoptosis in neuregulin-treated cells. To determine whether ring formation is due to cell movement, neuregulin-treated N87 cells were examined by time-lapse cinematography, which resolved temporal stages of this process (Figure 2, E–H). First, the compact multilayered colony became relatively flat, and the area occupied by the colony increased. Later, a gap appeared in the center of the colony (Figure 2F). The size of this gap gradually increased, resulting in the formation of a definitive ring (Figure 2G). Occasionally, we also observed ring formation by interaction between neighboring cells or cell aggregates (Figure 2H).

The process of ring formation could be modulated by changing ligand concentration. In the absence of ligand a very low frequency of spontaneous ring formation was observed (<1% of the colonies). By elevating ligand concentration, the number of ring-forming colonies increased, and the maximal level of ring formation (~90%) was obtained at 100 ng/ml ligand concentration. Rings formed as a result of neuregulin treatment were stable in 10% bovine calf serum-containing medium for a relatively long period (7 d).

To assess how general the morphogenetic reactions described above are, we examined neuregulin effects on several human epithelial lines of different origins. Among those were A431 (squamous cell carcinoma), DU 145 (prostate carcinoma), IGROV (ovarian cell carcinoma), and T47D and MCF7 (breast carcinomas). We found that all the cell lines studied react to the neuregulin treatment first by ring formation (Figures 3 and 10D), which could be followed by complete scattering. Some of these cell types formed well-developed, ring-shaped multicellular structures after relatively short (6 h) incubation with neuregulin (Figure 3), whereas others (MCF7 and majority of colonies of IGROV cells) underwent complete scattering during this time (our unpublished results). The ratios between the colonies that undergo conversion to the rings and those that undergo complete scattering varied with time after stimulation and were different in

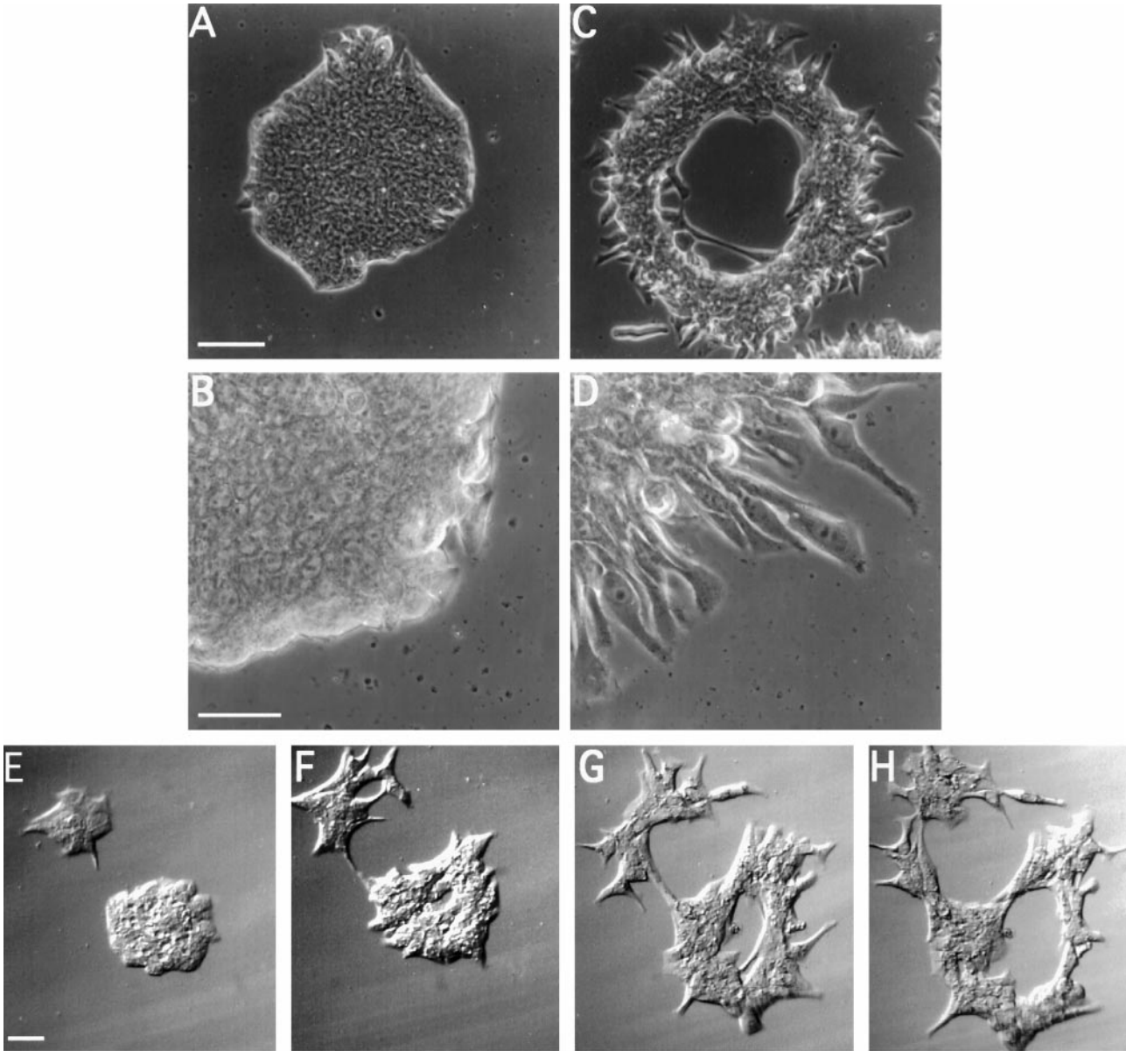

Figure 2. Neuregulin induces formation of the ring-shaped structures from the colonies of N87 cells. The cells were plated in serum containing medium for 4 d and then incubated in serum-free medium without (A and B) or with (C–H) NDF-β4 (100 ng/ml) for 3 d (C and D), 1 h (E), 24 h (F), 48 h (G), and 60 h (H). (E–H) Photographs of the same field. Note fully formed multicellular ring in C, activation of cell lamellipodial activity at the outer front of the ring in D, and temporal stages of ring-shaped structures formation in E–H. Bars, (A and C) 100 μm; (B and D) 50 μm; (E–H) 50 μm.

different cell lines. Thus, morphogenetic effects induced by neuregulin are general and characteristic for different types of epithelial cells.

Neuregulin Increases Cell Motility and Lamellipodial Activity

During both scattering and ring formation neuregulin induced a rapid increase in peripheral lamellipodial activity (Figure 2, compare B and D). This increase of lamellipodial activity was apparent as early as 10 min after neuregulin addition (our unpublished results). In the multicellular rings, two types of cell fronts were present, one facing the exterior of the ring and the other facing the interior. The "inner fronts" were smooth and essentially devoid of lamellipodial extensions, whereas the "outer fronts" were enriched with lamellipodial protrusions (Figure 2D) during the whole period of ring formation.

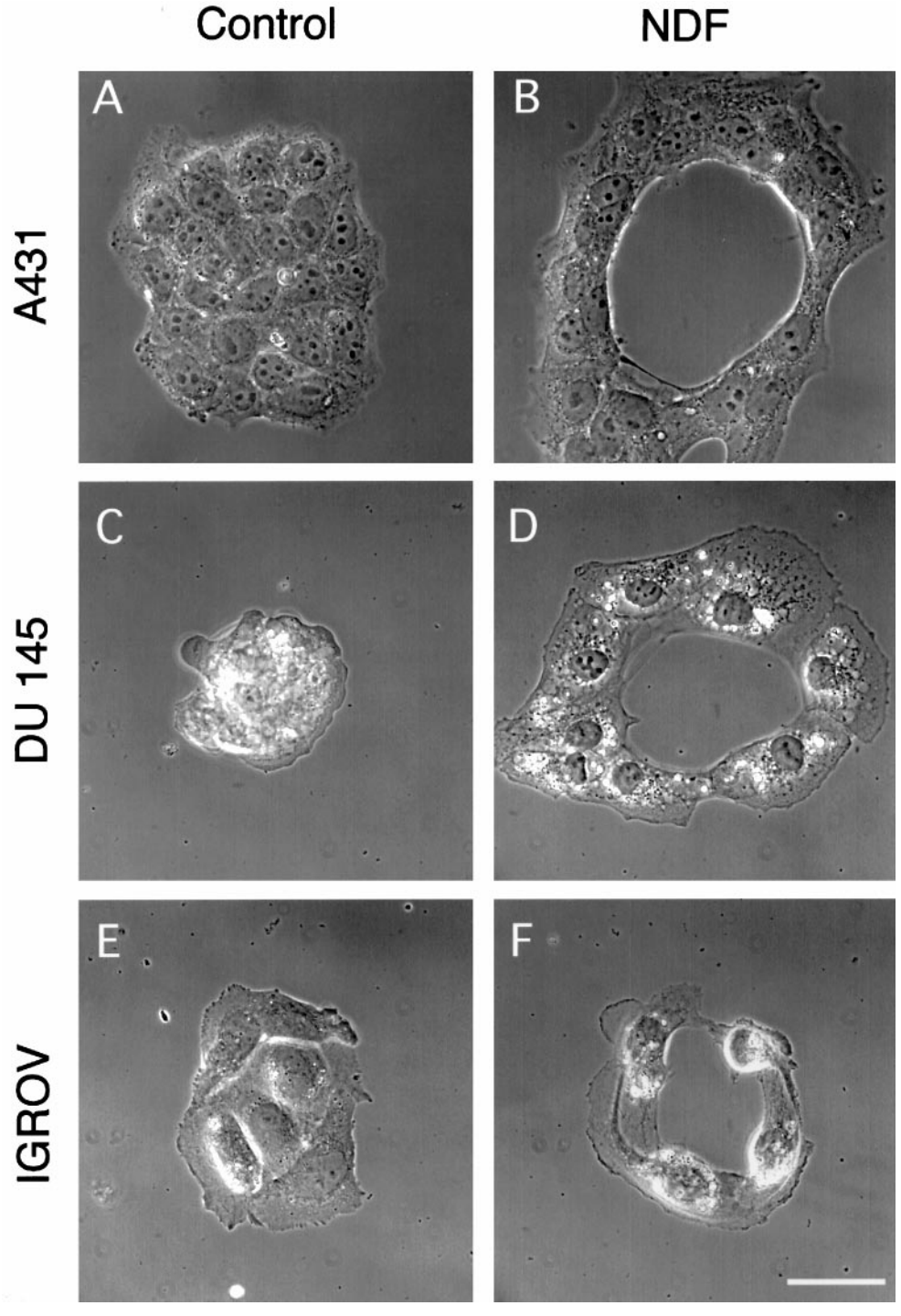

Figure 3. Neuregulin effects on different epithelial cell lines. Cells of squamous carcinoma A431 (A and B), prostate carcinoma DU 145 (C and D) and ovarian carcinoma IGROV (E and F) were plated at low density and maintained in serum-containing medium for 3 d. After formation of cell colonies (A, C, and E), the medium was changed to serum-free medium, and neuregulin (20 ng/ml) was added for an additional 6 h. The majority of colonies in the cultures of A431 and DU 145 cells were transformed into ring-shaped structures (B and D). Colonies of IGROV cells tended to undergo scattering but first formed some ring-shaped multicellular complexes (F). Note spreading of cell colonies and stimulation of lamellipodial activity at the outer front of the multicellular rings after neuregulin treatment (B, D, and F). Bar, 30 μm.

Stimulation of the lamellipodial extension suggests that cell motility is activated by neuregulin. To investigate whether neuregulin indeed elevates migratory activity, we measured the phagokinetic tracks formed by individual cells or small cell clusters. N87 cells were sparsely plated on the coverslips coated with colloidal gold particles, neuregulin was added 4 h after plating for additional 20 h, and the area of gold-free tracks formed by the moving cells was measured. As shown in Figure 4A, the control colonies cleared the underlying gold from only a relatively small area around them, suggesting that these epithelial cells are

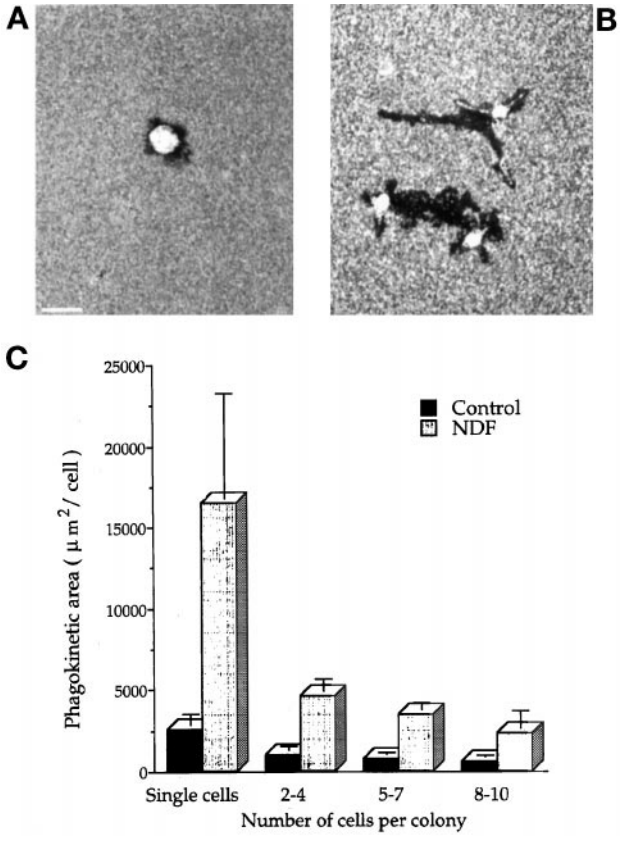

Figure 4. Neuregulin increases cell motility. The trajectories of control (A) and neuregulin-stimulated (20 ng/ml) (B) cells visualized by the phagokinetic track method are shown. The areas of the phagokinetic tracks formed by single cells and small cell colonies, normalized to the number of cells, are shown in C. Results of one typical experiment are presented; 50 tracks were measured for each experimental point. Two other experiments showed a similar effect. Bar (A and B), 100 μm.

essentially immobile. However, the size of the phagokinetic tracks formed by individual cells and small cell clusters in the neuregulin-treated cultures was significantly larger (Figure 4B). Individual cells demonstrated the strongest effect, increasing the average area of the tracks almost sevenfold as a result of neuregulin treatment. A similar tendency was observed with colonies containing up to 10 cells. These colonies typically showed a threefold increase in the phagokinetic track area (Figure 4C).

Organization of Cell–Cell Junctions and the Actin Cytoskeleton in Neuregulin-induced Rings

Using immunofluorescence microscopy, we examined the distribution of the major junctional proteins and actin in N87 cell cultures before and after neuregulin treatment. First, we showed that maturation of cell–cell junctions is necessary for the formation of the neuregulin-induced, ring-shaped multicellular structures. In particular, we found that colonies cultured for only 1 d before neuregulin treatment displayed weak cadherin staining in the cell–cell adherens junctions and diffuse distribution of desmoglein (Figure 5, A and D). These colonies underwent complete scattering after incubation with neuregulin (Figure 1C). On the other hand, colonies cultured for 3 d before neuregulin addition displayed high levels of junctional cadherin and desmoglein-positive spots in the areas of cell–cell contacts (Figure 5, B and E). Only these "mature" colonies underwent transformation into rings upon addition of neuregulin (Figures 1F and 5, C and F). Comparison of the distribution of junctional proteins in nontreated colonies and neuregulin-induced multicellular rings showed that both desmosomes and adherens junctions were not abolished during ring formation (Figures 5, C and F, and 6, B, D, and F). In particular, staining of the cells with antibodies against cadherin, β-catenin, and plakoglobin showed that these proteins were similarly associated with the cell–cell contacts in the ring-shaped structures, comparable with those found in nontreated colonies (Figure 6). Moreover, staining for β-catenin was more organized and enriched in cell–cell junctions of the rings (Figure 6, compare E and F). The intensity of cadherin and plakoglobin (but not of β-catenin) staining was slightly reduced in the fully developed rings (Figure 6, compare A with B and C with D), but cell–cell junctions were still prominently present.

Comparison of confocal images of the neuregulin-treated N87 cell colonies with those of control cells revealed some substantial changes in actin organization and general morphology. Control colonies consisted of several (3–4) layers of cells (Figure 7, A–C). The basal layer, which was attached to the substrate, contained actin cables (stress fibers) and relatively less developed cell–cell junctions (Figure 7, C and D). The cells in the suprabasal layers had essentially no stress fibers but showed highly developed, actin-rich cell–cell junctions (Figure 7B). The first apparent effect of neuregulin treatment was rapid spreading and flattening of the colonies. These changes were attributable to both flattening of cells in all layers as well as to a decrease in the number of cell layers (Figure 7, compare E with A). The cells in the basal layer increased their spreading area and developed numerous prominent stress fibers (Figure 7, G and H). The fraction of cells forming stress fibers increased in response to neuregulin. At the same time, actin staining of cell–cell contacts did not decrease in the neuregulin-induced rings (Figure 7, compare F with B).

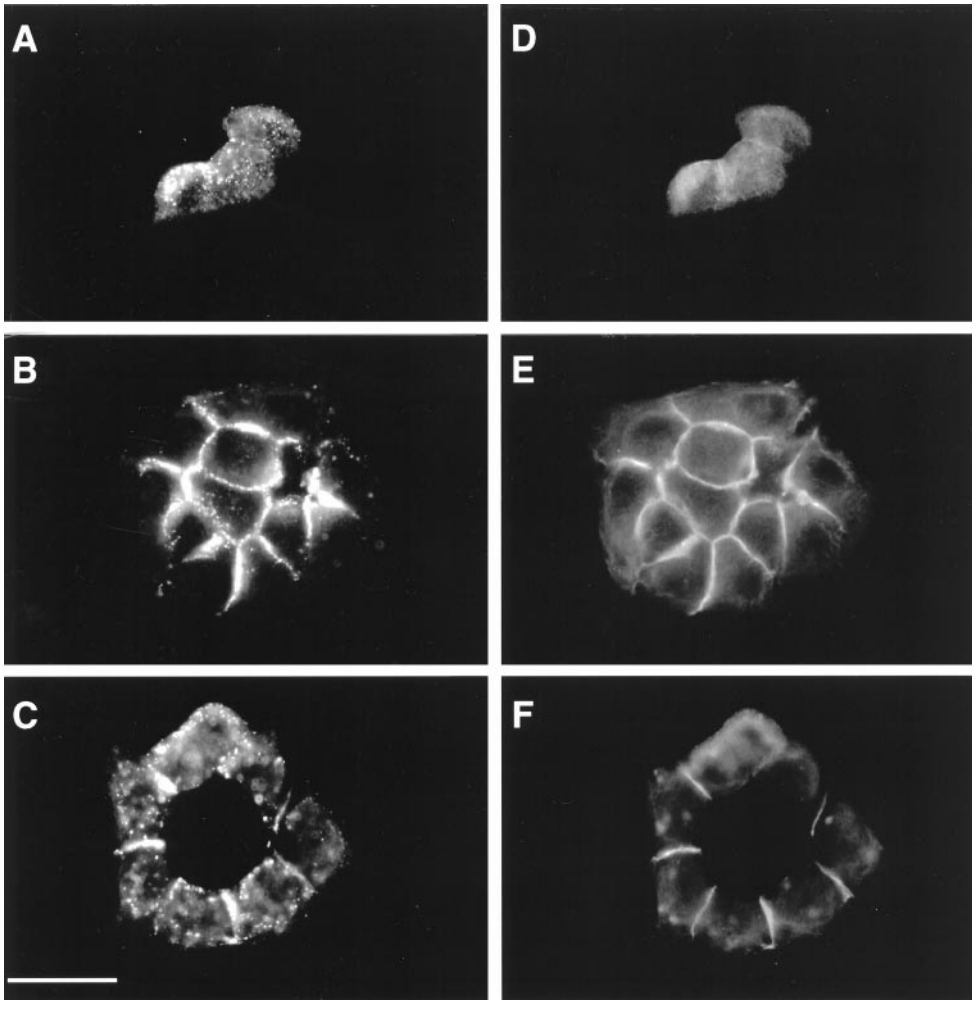

Figure 5. Maturation of cell–cell contacts in N87 cells as a function of time. Visualization of desmosomes by anti-desmoglein staining (A, B, and C) and of adherens junctions by anti-pan cadherin staining (D, E, and F) in the cell colonies 24 h (A and D) and 96 h (B and E) after plating. Note that after 24 h plating cells have dispersed single desmosomes and diffuse distribution of cadherin, whereas more prolonged cultivation resulted in condensation of both markers in the cell–cell junction areas (B and E). These mature cell colonies are converted into rings on an additional 48 h treatment with 100 ng/ml NDF (C, F). Bar, 30 μm.

Morphogenic Effect of Neuregulin Does Not Involve HGF/SF and c-Met Signaling

Because HGF/SF was shown to induce cell scattering in epithelial cells, we checked whether the neuregulin-mediated morphogenic effects are operating via the same pathway. We did not detect any HGF in the neuregulin sample, nor was neuregulin present in the HGF preparation (Figure 8). We were able to detect only a minor and transient increase in the c-Met tyrosine phosphorylation within 2 min after addition of neuregulin, whereas HGF treatment of the same cells resulted in strong and sustained phosphorylation of the c-Met receptor (Figure 9). The low level of phosphorylation of c-Met induced by neuregulin treatment is most likely insufficient for stimulation of cell scattering, because even a much higher degree of phosphorylation induced in similar cultures by HGF/SF treatment did not stimulate cell motility (the value of the aggregation index of N87 cells treated with HGF/SF was 4.1).

To further determine possible involvement of the c-Met receptor in neuregulin-induced morphogenic processes, we used a subline of T47D cells that does not express a detectable level of the c-Met receptor (Figure 10A). Yet, these cells do respond to neuregulin treatment similar to N87 cells by an increase of the migratory ability in the phagokinetic assay (Figure 10B) and by colony-to-ring conversion (Figure 10, C and D). HGF/SF, on the other hand, did not induce any effects in T47D. We therefore concluded that the c-Met receptor is not involved in the neuregulin-induced morphogenic effects.

Morphogenic Processes Induced by Neuregulin Are Mediated by ErbB-2 and -3 Heterodimers

Signaling by ErbB family receptors is triggered by ligand-induced receptor dimerization (Yarden and Schlessinger, 1987; Cochet *et al.*, 1988; Lee *et al.*, 1989; Lehvaslaiho *et al.*, 1989; Ullrich and Schless-

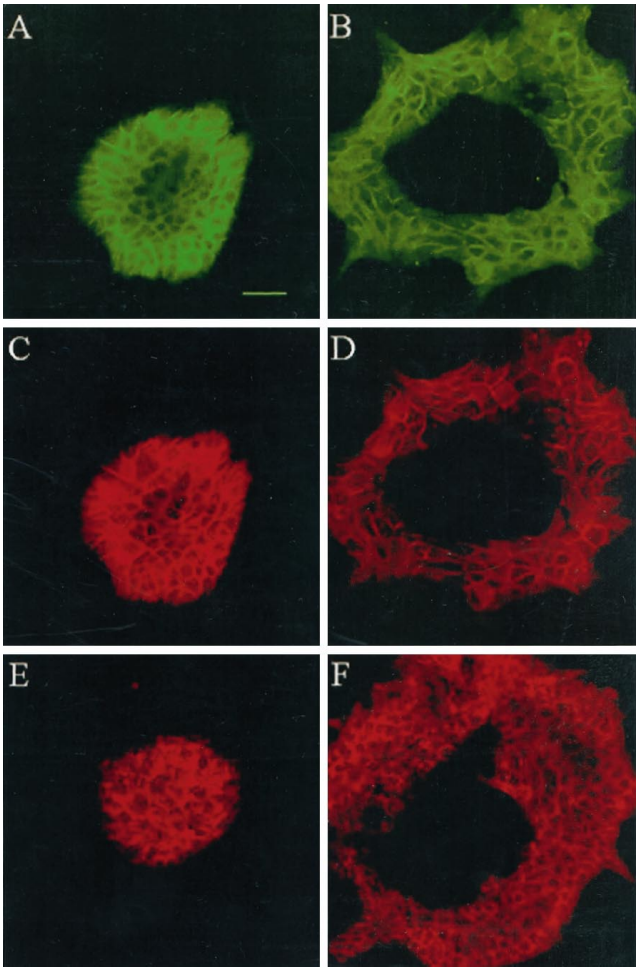

Figure 6. Adherens junction proteins in control cell colonies (A, C, and E) and ring-shaped structures formed on neuregulin treatment for 3 d (B, D, and F). Cells were stained with antibody against pan-cadherin (A and B), plakoglobin (C and D), and β-catenin (E and F). (A and C and B and D), Pairs corresponding to the same fields. Bar, 50 μm. Note the good preservation of cell adherens junctions in ring-shaped multicellular structures (B, D, and F) and some decrease in cadherin and plakoglobin staining in the ring (B and D) compared with control colony (A and C).

inger, 1990). We analyzed the receptor subtype expression in N87 and T47D lines (Figure 11A). It was shown that T47D cells express all four members of the ErbB family, whereas N87 expresses ErbB-1, -2, and -3. To determine which of the homodimers or heterodimers is involved in the neuregulin-induced morphological changes, N87 cells were stimulated with radiolabeled neuregulin, and the bound ligand

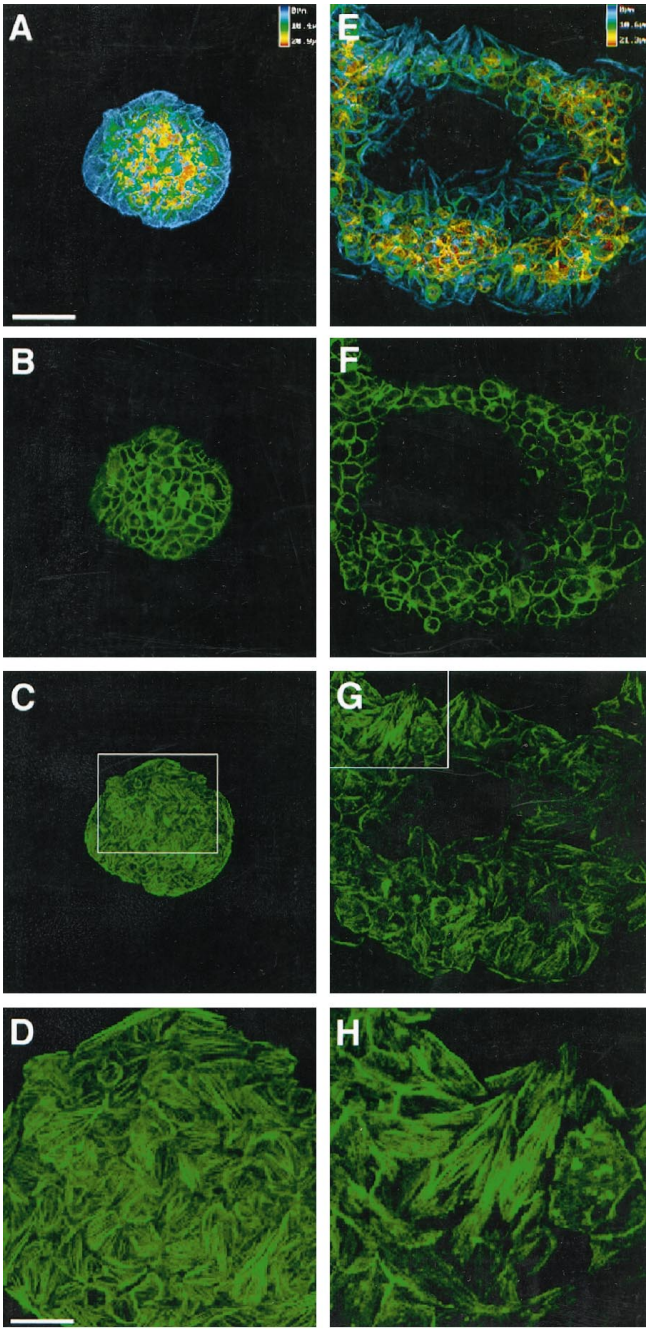

colors are arranged in "spectral" order so that red corresponds to the objects distant from the substrate (~20 μm), and violet–dark blue corresponds to the objects adjacent to the substrate (0–1 μm). The optical sections corresponding to one of the intermediate levels (12 μm from the substrate) and to the substrate-adjacent level are shown in B and F and C and G, respectively. The regions of the basal cell layers marked by boxes in C and G are shown with higher magnification in D and H. Bars, (A–C and E–G) 50 μm (shown in A); (D and H) 20 μm (shown in D). Note the flattening of cell colonies during ring formation (E compared with A) and increase of the size of actin cables in basal cell layer (H compared with D). Cells in the upper layers of colonies and rings display F-actin mainly in the cell–cell junctions (B and F).

Figure 7. Confocal images of the actin staining in control cell colony (A–D) and in multicellular ring formed after 100 ng/ml NDF treatment for 3 d (E–H). In A and E the distance of the cells from the substrate plane is shown by the depth coding in pseudocolors. The

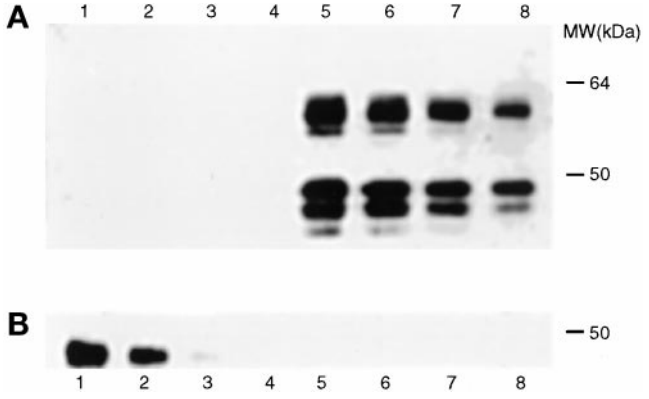

Figure 8. Western blotting determination of HGF/SF and neuregulin content in culture medium. Lanes 1–4 correspond to the medium containing 200, 100, 50, and 10 ng/ml NDF-β4. Lanes 5–8 correspond to dilutions of 1:1, 1:2, 1:4, and 1:8 of HGF/SF-conditioned medium. The media were precipitated with heparin-Sepharose, separated by SDS-gel electrophoresis, and immunoblotted with anti-HGF (A) and anti-neuregulin (B) antibodies, respectively. Neither contamination of the NDF-β4 preparation by HGF/SF nor any traces of NDF-β4 in HGF/SF-conditioned medium were detected. Even the highest concentration of HGF/SF easily detected by the present method did not induce scattering of N87 cells.

was chemically cross-linked to the receptors and immunoprecipitated with anti-receptor antibodies. The receptors that form direct or trans complexes with neuregulin were visualized by autoradiography. As a control for binding specificity, we carried out neuregulin binding in the presence of excess unlabeled ED NDF-β1. These cross-linking experiments revealed two populations of neuregulin-bound ErbB receptors in cell lysates, corresponding to monomeric and dimeric forms (Figure 11B). The molecular composition of these complexes was further determined by immunoprecipitation with specific antibodies to the four ErbB receptors, indicating that the ErbB-2 and -3 complex was the only prominent heterodimer formed (Figure 11C).

To determine whether activation of the ErbB-2 and -3 complex by neuregulin is sufficient for the induction of the morphogenic effects, we added the ligand to CHO cells expressing specific combinations of ErbB receptors on a low background of the endogenous hamster ErbB-2. These include CB-1 cells (expressing ErbB-1), CB-2 (expressing ErbB-2), CB-3 (expressing ErbB-3), CB-4 (expressing ErbB-4) (Tzahar *et al.*, 1996), and NEC cells expressing an ErbB-1 and -2 chimeric receptor (Peles *et al.*, 1992). Because CHO cells contain very low levels of cadherin and thus do not form coherent colonies and stable cell–cell junctions, we could not study scattering or ring formation in experiments with these cells. We were able, however, to detect a strong morphogenic response (cavity formation) upon stimulation of dense cultures of CB-3 cells with the neuregulin (Figure 12F). These cells, containing ErbB-3 and the endogenous hamster ErbB-2 but none of the other cell lines treated with corresponding ligands, formed prominent cavities (Figure 12). In conclusion, coexpression of ErbB-2 and -3 is sufficient for at least part of the morphogenic effect of NDF, supporting the idea that the ErbB-2 and -3 heterodimers mediate the neuregulin-induced morphogenesis.

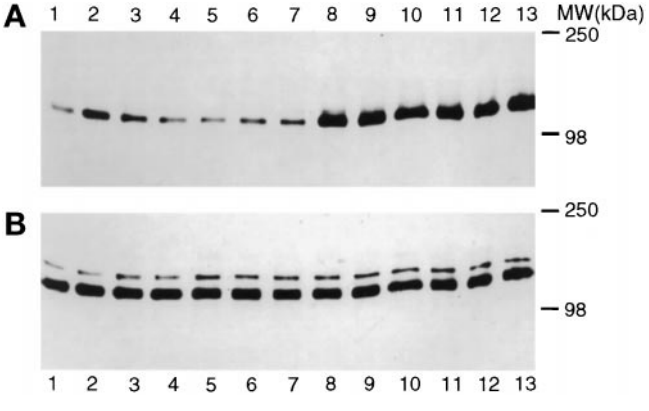

Figure 9. Activation of c-Met receptor by HGF/SF and neuregulin treatment. Control N87 cells (lane 1) and the same cells activated with 10 ng/ml NDF-β4 (lanes 2–7) or with a 1:2 dilution of HGF-conditioned medium (lanes 8–13) for 1 min (lanes 2 and 8), 2 min (lanes 3 and 9), 5 min (lanes 4 and 10), 10 min (lanes 5 and 11), 30 min (lanes 6 and 12), and 60 min (lanes 7 and 13) were lysed, immunoprecipitated with anti-c-Met antibodies, and immunoblotted with anti-phosphotyrosine (A) or anti-c-Met antibodies (B). Note that NDF-β4 stimulation induced only a weak and transient increase in tyrosine phosphorylation of c-Met receptor compared with HGF/SF treatment of the same cells.

DISCUSSION

In the present study we demonstrate for the first time that neuregulin can induce specific morphogenic effects in cultured epithelial cells. These responses include activation of cell locomotion leading to the scattering or disintegration of small epithelial islands or the formation of unique, ring-shaped colonies by larger epithelial islands. In dense monolayers neuregulin induced the formation of lumenlike structures.

What are the cellular changes underlying the morphogenetic processes induced by neuregulin? As shown here, neuregulin is a strong epithelial motogen stimulating the motility not only of individual cells, but also of small colonies. Cell motility is a complex process that depends on several classes of cellular events, including lamellipodial extension, substrate adhesion, and cell contractility (Bray, 1992). We observed increased lamellipodial activity within 10 min after addition of neuregulin that persisted throughout the scattering or ring formation process.

The involvement of specific changes in cell–substratum adhesion in neuregulin-induced morphogenesis

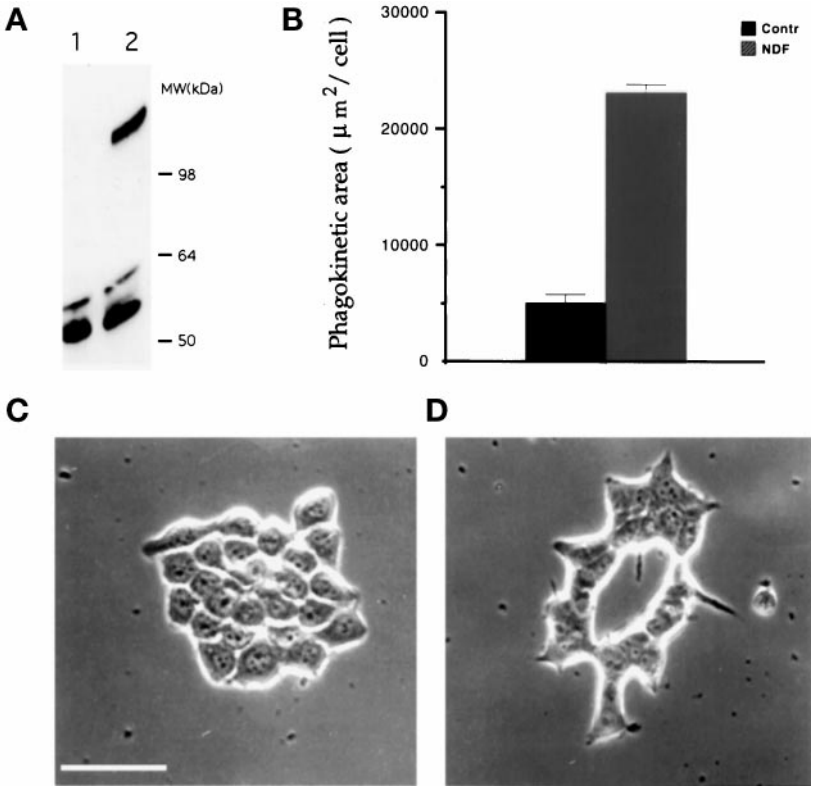

Figure 10. Neuregulin induces motogenic and morphogenic effects in T47D cells lacking c-Met receptor. (A) T47D (lane 1) and N87 (lane 2) cell lysates were immunoprecipitated with anti-c-Met antibodies, separated by SDS-gel electrophoresis, and immunoblotted with the same antibodies. Only N87 cells show the positive band corresponding to c-Met protein. The low-molecular-weight bands correspond to the heavy chain of the antibodies. (B) Areas of the phagokinetic tracks of single T47D cells not treated or treated with 20 ng/ml NDF. Fifty tracks were measured for each experimental point. (C) Control colony of T47D cells. (D) Ring-shaped multicellular structure formed by T47D cells treated with NDF-β4. Bar, 100 μm.

was not directly investigated in this study; nevertheless, it was noted that changes in the tissue culture substratum had an effect on the morphogenic response. Thus, scattering and ring formation were readily obtained when cells were cultured on glass coverslips but were hardly detectable when the same cells were cultured on tissue culture plastic (our unpublished results). Interestingly, a similar dependence on the substrate was also observed for the HGF/SF effect. In this case, however, efficient scattering occurs on a tissue culture plastic surface, whereas adhesion to a glass surface interfered with the effect (Clark, 1994). It was also shown that attachment to vitronectin prevents the scattering effect of HGF/SF, whereas fibronectin allows it (Clark, 1994). Moreover, physical properties of the ECM can significantly modulate the effect of HGF/SF signaling. It has been shown that patterns of cell scattering and morphogenesis induced by HGF/SF were distinctly different when cells were cultured in three-dimensional matrix compared with two-dimensional tissue culture surfaces (Montesano *et al.*, 1991; Soriano *et al.*, 1995). The potential cross-talk between neuregulin signaling and ECM-mediated signaling requires further study.

Because the morphological alterations induced by neuregulin are similar to those previously described for HGF/SF (Stoker *et al.*, 1987; Tsarfaty *et al.*, 1992), we examined the possibility that HGF/SF is also involved in the cell scattering and induction of luminal structures by neuregulin. It was found in this study that c-Met was not significantly tyrosine phosphorylated after neuregulin stimulation. Furthermore, we found that a subline of T47D cells that does not express c-Met protein responds fully to neuregulin. Individual cells treated with the neuregulin became more motile, whereas cell colonies underwent transformation to the ring-shaped structures. Thus, morphogenic effects of neuregulin in our cells are not mediated by HGF/SF and c-Met signaling.

Are there specific alterations in cell–cell contacts induced by neuregulin? As already mentioned, it was shown that classical SFs disrupt desmosomes and destabilize cadherin-mediated cell–cell junctions (Watabe *et al.*, 1993; Savagner *et al.*, 1997; Potempa and Ridley, 1998). Obviously, complete scattering of immature, small colonies leads to the loss of intercellular junctions, yet we have no evidence that down-regulation of cell–cell junctions is involved in neuregulin response. The possibility that loss of cell junction is secondary to increased cell motility is supported by the fact that neuregulin treatment of mature cell colonies with well-developed adherens junctions and desmosomes does not induce major disruption of these contact structures. Thus, it may be proposed that the response of cell colonies to neuregulin treatment involves changes in the fine balance between locomo-

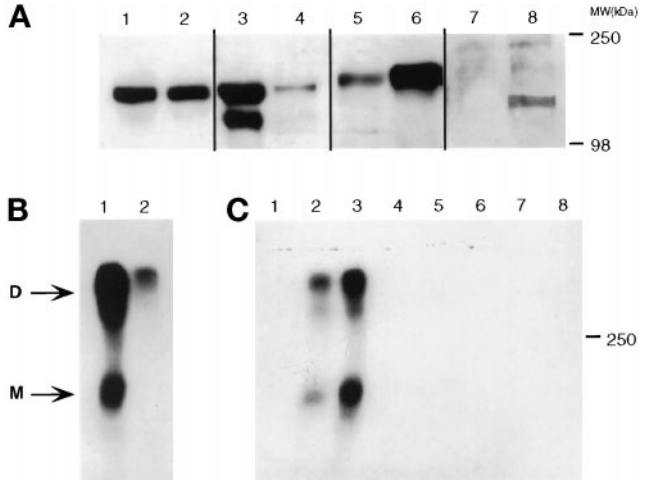

Figure 11. Interaction of neuregulin with ErbB family receptors in T47D and N87 cells. (A) The lysate of N87 (lanes 1, 3, 5, and 7) and T47D (lanes 2, 4, 6, and 8) cells were immunoprecipitated with anti-ErbB-1 (lanes 1 and 2), -2 (lanes 3 and 4), -3 (lanes 5 and 6), and -4 (lanes 7 and 8) antibodies, SDS-gel electrophoresed, and immunoblotted with the polyclonal antibodies of the same specificity, respectively. (B) N87 cells were incubated with iodinated ^{125}I-labeled NDF-β4 (10 ng/ml) without (lane 1) or with (lane 2) a 100-fold excess of the unlabeled ED NDF-β1. The N87 cells were then washed with PBS, treated with disuccinimidyl suberate cross-linker, lysed, SDS-gel electrophoresed, and autoradiographed. The bands corresponding to receptor monomers (M) and dimers (D) are shown. (C) N87 cells were incubated with iodinated ^{125}I-labeled NDF-β4 without (lanes 1–4) or with (lanes 5–8) a 100-fold excess of unlabeled ED NDF-β1. After cross-linker treatment and cell lysis, the lysates were immunoprecipitated with anti-ErbB-1 (lanes 1 and 5), -2 (lanes 2 and 6), -3 (lanes 3 and 7), and -4 (lanes 4 and 8) antibodies, followed by SDS-gel electrophoresis and autoradiography. Bands corresponding to the binding of ^{125}I-labeled NDF-β4 to the receptors precipitated by anti-ErbB-2 and -3 antibodies are clearly seen (lanes 2 and 3).

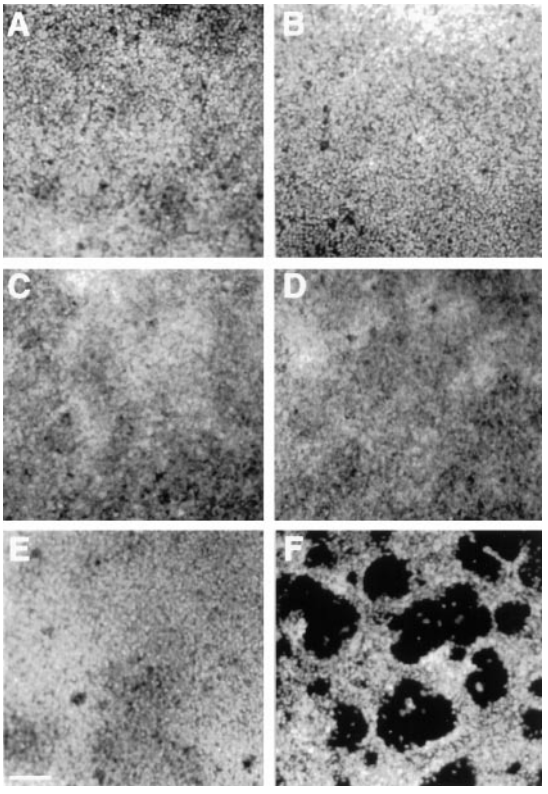

Figure 12. Activation of different combinations of ErbB family receptors in CHO cells. CHO cells expressing endogenously only ErbB-2 receptor were stably transfected with ErbB-1 (CB-1 line), ErbB-2 (CB-2 line), ErbB-3 (CB-3 line), ErbB-4 (CB-4 line), and EGFR-ErbB-2 chimera (NEC line). Dense monolayers of CB-1 (A), CB-2 (B), NEC (C), CB-4 (D), and CB-3 (E and F) were treated with EGF (A and C), anti-ErbB-2 antibody (B), or β4 NDF (D and F) or left untreated (E). Cells were stained with DAPI. Scale bar, 100 μm. Only CB-3 cells treated with β4 NDF showed formation of numerous cavities in the monolayer (F).

tion and cell–cell junction formation. Immature colonies with relatively poor junctions undergo complete scattering, whereas more mature colonies with well-developed junctions transform into the ring-shaped structures. In different cell lines the neuregulin treatment resulted in different ratios between rings and completely scattered colonies depending on the levels of cell–cell adhesion in these cultures. Thus the simplest model explaining the observed effects of neuregulin does not require a direct effect of neuregulin on either desmosomes or adherens junctions. Taken together, our data show that the state of the culture before neuregulin treatment significantly affects the final result of this activation. Moreover, these results suggest that formation of complex multicellular structures can be a result of the shift in a balance between adhesion and motility induced by extracellular ligand.

Which receptors are involved in the transduction of the neuregulin-induced morphogenic signals? Based on previous data, neuregulin can bind to either ErbB-3 or -4 (Tzahar *et al.*, 1994). Our results indicate that in N87 cells neuregulin interacts with ErbB-3 and induces the formation of heterodimers with ErbB-2. The suggestion that ErbB-2 and -3 comprise the active receptor species involved in neuregulin-induced morphogenesis is based on the idea that ligands reacting with ErbB family members can induce receptor dimerization. Because ErbB-2 is considered an "orphan receptor" and does not directly interact with neuregulin, and because the catalytic function of ErbB-3 is defective and cannot signal by itself (Burden and Yarden, 1997), we propose that binding of neuregulin to ErbB-3 induces formation of signaling heterodimers with ErbB-2, which in turn, triggers the response. The ability of ErbB-2 to act in a cooperative manner with other ErbB proteins as a shared, low-affinity receptor (coreceptor) for multiple stroma-derived growth factors is well established and plays an important role in oncogenic function of this receptor in epithelial tumors (Tzahar and Yarden, 1998).

What are the molecular targets of ErbB-2 and -3-mediated signals that are responsible for the morphogenic events? Although this aspect was not directly investigated here, it is noteworthy that one of the major pathways stimulated by receptor tyrosine kinases, including the ErbB family, involves activation of MAP kinase (Erk1 and Erk2) (Burden and Yarden, 1997). MAP kinase activation, in turn, can affect cell motility by enhancing the myosin light-chain kinase activity and consequent increase of cell contractility (Klemke *et al.*, 1997). Another target of ErbB-2 and -3 signaling related to the regulation of cell motility is phosphatidylinositol 3-kinase. This kinase was shown to be activated by ErbB-2 (Peles *et al.*, 1992) and ErbB-3 (Carraway *et al.*, 1995; Tansey *et al.*, 1996) and, in turn, can interact with Rac GTPase, thereby increasing cell lamellipodial activity (Bokoch *et al.*, 1996; Reif *et al.*, 1996).

Several previous lines of evidence support the involvement of neuregulin signaling in the regulation of organogenesis in vivo. First, the neuregulin-deficient mice as well as mice lacking ErbB-2 or -4 demonstrated lethal defects caused by abnormal heart development. The morphogenic phase of trabeculae formation did not occur in all three mutant mice (Gassmann *et al.*, 1995; Lee *et al.*, 1995; Meyer and Birchmeier, 1995). ErbB-3(−/−) mice display defects in atrioventricular valve formation (Erickson *et al.*, 1997) as well as severe neuropathies caused by loss of Schwann cells that accompany peripheral axons of sensory and motor neurons (Riethmacher *et al.*, 1997). The reason why epithelial defects are not prominently detectable in neuregulin-targeted mice is not clear but may be due to early embryonic death of the mutant mice or a relatively late onset of epithelial organogenesis (Burden and Yarden, 1997). However, ErbB-3(−/−) mice already display some abnormalities in stomach and pancreas development (Erickson *et al.*, 1997).

In this work we showed for the first time that neuregulin can induce via ErbB-2 and -3 receptors specific changes in motility and morphogenetic behavior of cultured epithelial cells. Our results are in agreement with recent studies showing that neuregulin treatment induces formation of lobular–alveolar structures in organ cultures of mammary glands (Yang *et al.*, 1995; Jones *et al.*, 1996). We were able to demonstrate that the primary effect underlying the morphogenetic changes induced by neuregulin is an increase of cell motility. This is again in agreement with the results demonstrating the role of neuregulin signaling in another cellular model, development of the sympathetic nervous system. Experiments with targeted mutations in the ErbB-2 and -3 or neuregulin-1 genes show that neuregulin and ErbB-2 and -3 signaling is essential for the migration of the neural crest cells (Britsch *et al.*, 1998). Neuregulins were shown to up-regulate motility of Schwann cells (Mahanthappa *et.al.*, 1996) and epidermal migration (Danilenko *et al.*, 1995). Together these results indicate that the neuregulin and ErbB-3 and -2 pathway is a powerful inducer of cell motility. The effect of this signaling in epithelial cells, however, differs from the effect of another potent motogen, HGF/SF; destabilization of cell–cell adhesions is less pronounced in the case of neuregulin, and therefore the balance between increased motility and preserved cell–cell adhesion leads to formation of unique multicellular structures, even in conditions of monolayer culture. HGF/SF, on the other hand, can form branching tubular structures mainly in three-dimensional cultures in collagen. It is interesting that in a physiological situation, for example in mammary gland development, both signaling pathways are involved (Yang *et al.*, 1995), showing that the corresponding morphogenetic effects are complementary.

In the present work we studied only neoplastically transformed epithelial cells. All the carcinomas studied were shown to be sensitive to the morphogenic effects induced by neuregulin. It is known that enhancement of c-Met signaling in many cases correlates with metastatic potential of transformed cells (Vande Woude *et. al.*, 1997). One can suggest that alteration of the fine balance between cell–cell adhesion and autonomous cell motility induced by the neuregulin and ErbB-3 and -2 pathway might also be one of the factors promoting carcinoma metastasis. In this connection it is interesting that ErbB-2 and -3 overexpression correlates with high malignancy and metastatic potential (Myers *et al.*, 1994).

ACKNOWLEDGMENTS

This study was supported by grants from the Minerva Foundation (Munich, Germany), the Israel Science Foundation, The Israel Ministry of Science, the Crown Endowment Fund (to A.D.B.), and the Israel Science Foundation and the Rita Marcus Foundation (to B.G.). B.G. holds the E. Neter chair in Cell and Tumor Biology.

REFERENCES

Birchmeier, W., and Birchmeier, C. (1995). Epithelial-mesenchymal transition in development and tumor progression. In: Epithelial-Mesenchymal Interactions in Cancer, ed. I.D. Goldberg and E.M. Rosen, Basel: Birkhäuser Verlag, 1–15.

Bokoch, G.M., Vlahos, C.J., Wang, Y., Knaus, U.G., and Traynor-Kaplan, A.E. (1996). Rac GTPase interacts specifically with phosphatidylinositol 3-kinase. Biochem. J. *315*, 775–779.

Bottaro, D.P., Rubin, J.S., Faletto, D.L., Chan, A.M., Kmiecik, T.E., Vande Woude, G.F., and Aaronson, S.A. (1991). Identification of the hepatocyte growth factor receptor as the c-met proto-oncogene product. Science *251,* 802–804.

Boyer, B., Valles, A.M., Tucker, G.C., Delouvee, A., and Thiery, J.P. (1993). Involvement of cell motility in tumor progression. Symp. Soc. Exp. Biol. *47*, 183–195.

Bray, D. (1992). Cell Movements, New York: Garland Publishing.

Britsch, S., Li, L., Kirchhoff, S., Theuring, F., Brinkmann, V., Birchmeier, C., and Riethmacher, D. (1998). The ErbB2 and ErbB3 recep-

tors and their ligand, neuregulin-1, are essential for development of the sympathetic nervous system. Genes Dev. *12,* 1825–1836.

Burden, S., and Yarden, Y. (1997). Neuregulins and their receptors: a versatile signaling module in organogenesis and oncogenesis. Neuron *18*, 847–855.

Carraway, K.L., III, Soltoff, S.P., Diamonti, A.J., and Cantley, L.C. (1995). Heregulin stimulates mitogenesis and phosphatidylinositol 3-kinase in mouse fibroblasts transfected with erbB2/neu and erbB3. J. Biol. Chem. *270*, 7111–7116.

Clark, P. (1994). Modulation of scatter factor/hepatocyte growth factor activity by cell-substratum adhesion. J. Cell Sci. *107*, 1265–1275.

Cochet, C., Kashles, O., Chambaz, E.M., Borrello, I., King, C.R., and Schlessinger, J. (1988). Demonstration of epidermal growth factor-induced receptor dimerization in living cells using a chemical crosslinking agent. J. Biol. Chem. *263*, 3290–3295.

Danilenko, D.M., Ring, B.D., Lu, J.Z., Tarpley, J.E., Chang, D., Liu, N., Wen, D., and Pierce, G.F. (1995). Neu differentiation factor upregulates epidermal migration and integrin expression in excisional wounds. J. Clin. Invest. *95*, 842–851.

Erickson, S., Shea, K., Ghaboosi, N., Loverro, L., Frantz, G., Bauer, M., Lu, L., and Moore, M. (1997). ErbB3 is required for normal cerebellar and cardiac development: a comparison with ErbB2- and heregulin-deficient mice. Development *124*, 4999–5011.

Gassmann, M., Casagranda, F., Orioli, D., Simon, H., Lai, C., Klein, R., and Lemke, G. (1995). Aberant neural and cardiac development in mice lacking the ErbB4 neuregulin receptor. Nature *378*, 390–394.

Gherardi, E., Sharpe, M., Lane, K., Sirulnik, A., and Stoker, M. (1993). Hepatocyte growth factor/scatter factor (HGF/SF), the c-met receptor and the behavior of epithelial cells. Symp. Soc. Exp. Biol. *47*, 163–181.

Hay, E.D. (1995). An overview of epithelio-mesenchymal transformation. Acta Anat. *154*, 8–20.

Jones, F.E., Jerry, D.J., Guarino, B.C., Andrews, G.C., and Stern, D.F. (1996). Heregulin induces in vivo proliferation and differentiation of mammary epithelium into secretory lobuloalveoli. Cell Growth Differ. *7*, 1031–1038.

Keydar, I., Chen, L., Karby, S., Weiss, F.R., Delarea, J., Radu, M., Chaitcik, S., and Brenner, H.J. (1979). Establishment and characterization of a cell line of human breast carcinoma origin. Eur. J. Cancer *15*, 659–670.

Kjelsberg, C., Sakurai, H., Spokes, K., Birchmeier, C., Drummond, I., Nigam, S., and Cantley, L.G. (1997). Met−/− kidneys express epithelial cells that chemotax and form tubules in response to EGF receptor ligands. Am. J. Physiol. *272*, F222–F228.

Klemke, R.L., Cai, S., Giannini, A.L., Gallagher, P.J., Lanerolle, P., and Cheresh, D.A. (1997). Regulation of cell motility by mitogen-activated protein kinase. J. Cell Biol. *137*, 481–492.

Lee, J., Dull, T.J., Lax, I., Schlessinger, J., and Ullrich, A. (1989). HER-2 cytoplasmic domain generates normal mitogenic and transforming signals in a chimeric receptor. EMBO J. *8*, 167–173.

Lee, K.F., Simon, H., Chen, H., Bates, B., Hung, M.C., and Hauser, C. (1995). Requirement for neuregulin receptor erbB2 in neural and cardiac development. Nature *378*, 394–398.

Lehvaslaiho, H., Lehtola, L., Sistonen, L., and Alitalo, K. (1989). A chimeric EGF-R-neu proto-oncogene allows EGF to regulate neu tyrosine kinase and cell transformation. EMBO J. *8*, 159–166.

Ma, J., Maliepaard, M., Kolker, H.J., Verweij, J., and Schellens, J.H. (1998). Abrogated energy-dependent uptake of cisplatin in a cisplatin-resistant subline of the human ovarian cancer cell line IGROV-1. Cancer Chemother. Pharmacol. *41*, 186–192.

Mahanthappa, N.K., Anton, E.S., and Matthew, W.D. (1996). Glial growth factor 2, a soluble neuregulin, directly increases Schwann cell motility and indirectly promotes neurite outgrowth. J. Neurosci. *16*, 4673–4683.

Meyer, D., and Birchmeier, C. (1995). Multiple essential function of neuregulin in development. Nature *378*, 386–390.

Montesano, R., Matsumoto, K., Nakamura, T., and Orci, L. (1991). Identification of a fibroblast-derived epithelial morphogen as hepatocyte growth factor. Cell *67*, 901–908.

Myers, R.B., Srivastava, S., Oelschlager, D.K., and Grizzle, W.E. (1994). Expression of p160erbB-3 and p185erbB-2 in prostatic intraepithelial neoplasia and prostatic adenocarcinoma. J. Natl. Cancer Inst. *86*, 1140–1145.

Naldini, L., *et al.* (1991). Scatter factor and hepatocyte growth factor are indistinguishable ligands for the MET receptor. EMBO J. *10*, 2867–2878.

Park, J.G., *et al.* (1990). Characteristics of cell lines established from human gastric carcinoma. Cancer Res. *50*, 2773–2780.

Peles, E., Lamprecht, R., Ben-Levy, R., Tzahar, E., and Yarden, Y. (1992). Regulated coupling of the Neu receptor to phosphatidylinositol 3′-kinase and its release by oncogenic activation. J. Biol. Chem. *267*, 12266–12274.

Pielou, E.C. (1969). An Introduction to Mathematical Ecology, New York: John Wiley & Sons.

Potempa, S., and Ridley, A.J. (1998). Activation of both MAP kinase and phosphatidylinositide 3-kinase by ras is required for hepatocyte growth factor/scatter factor-induced adherens junction disassembly. Mol. Biol. Cell *9*, 2185–2200.

Reif, K., Nobes, C.D., Thomas, G., Hall, A., and Cantrell, D.A. (1996). Phosphatidylinositol 3-kinase signals activate a selective subset of Rac/Rho-dependent effector pathways. Curr. Biol. *6*, 1445–1456.

Riethmacher, D., Sonnenberg-Riethmacher, E., Brinkmann, V., Yamaai, T., Levin, G., and Birchmeier, C. (1997). Severe neuropathies in mice with targeted mutations in the ErbB3 receptor. Nature *389*, 725–730.

Rong, S., Oskarsson, M., Faletto, D., Tsarfaty, I., Resau, J.H., Nakamura, T., Rosen, E., Hopkins, R.F., and Vande Woude, G.F. (1993). Tumorigenesis induced by coexpression of human hepatocyte growth factor and the human met protooncogene leads to high levels of expression of the ligand and receptor. Cell Growth Differ. *4*, 563–569.

Sachs, M., Weidner, K.M., Brinkmann, V., Walther, I., Obermeier, A., Ullrich, A., and Birchmeier, W. (1996). Motogenic and morphogenic activity of epithelial receptor tyrosine kinases. J. Cell Biol. *135*, 1095–1107.

Savagner, P., Boyer, B., Valles, A.M., Jouanneau, J., and Thiery, J.P. (1994). Modulations of the epithelial phenotype during embryogenesis and cancer progression. In: Mammary Tumorigenesis and Malignant Progression, ed. R. Dickson and M. Lippman, Norwell, MA: Kluwer Academic, 229–249

Savagner, P., Yamada, K., and Thiery, J. (1997). The zink-finger protein slug causes desmosome dissociation, an initial and necessary step for growth factor-induced epithelial-mesenchymal transition. J. Cell Biol. *137*, 1403–1419.

Soriano, J.V., Pepper, M.S., Nakamura, T., Orci, L., and Montesano, R. (1995). Hepatocyte growth factor stimulates extensive development of branching duct-like structures by cloned mammary gland epithelial cells. J. Cell Sci. *108*, 413–430.

Stoker, M., Gherardi, E., Perryman, M., and Gray, J. (1987). Scatter factor is a fibroblast-derived modulator of epithelial cell mobility. Nature *327*, 239–242.

Stone, K.R., Mickey, D.D., Wunderli, H., Mickey, G.H., and Paulson, D.F. (1978). Isolation of a human prostate carcinoma cell line (DU 145). Int. J. Cancer *21*, 274–281.

Tamagnone, L., and Comoglio, P.M. (1997). Control of invasive growth by hepatocyte growth factor (HGF) and related scatter factors. Cytokine Growth Factor Rev. *8*, 129–142.

Tansey, M.G., Chu, G.C., and Merlie, J.P. (1996). ARIA/HRG regulates AChR epsilon subunit gene expression at the neuromuscular synapse via activation of phosphatidylinositol 3-kinase and Ras/MAPK pathway. J. Cell Biol. *134*, 465–476.

Trinkaus, J.P. (1984). Cells into Organs: The Forces That Shape the Embryo, Englewood Cliffs, NJ: Prentice-Hall.

Tsarfaty, I., Resau, J.H., Rulong, S., Keydar, I., Faletto, D., and Vande Woude, G.F. (1992). The met proto-oncogene and lumen formation. Science *257*, 1258–1261.

Tsarfaty, I., Rong, S., Resau, J.H., Rulong, S., da Silva, P.P., and Vande Woude, G.F. (1994). The Met proto-oncogene mesenchymal to epithelial cell conversion. Science *263*, 98–101.

Tzahar, E., *et al.* (1994). ErbB-3 and ErbB-4 function as the respective low and high affinity receptors of all Neu differentiation factor/heregulin isoforms. J. Biol. Chem. *269*, 25226–25233.

Tzahar, E., Waterman, H., Chen, X., Levkowitz, G., Karunagaran, D., Lavi, S., Ratzkin, B.J., and Yarden, Y. (1996). A hierarchical network of interreceptor interactions determines signal transduction by Neu differentiation factor/neuregulin and epidermal growth factor. Mol. Cell. Biol. *16*, 5276–5287.

Tzahar, E., and Yarden, Y. (1998). The ErbB-2/HER2 oncogenic receptor of adenocarcinomas: from orphanhood to multiple stromal ligands. Biochim. Biophys. Acta *1377*, M25–M37.

Ullrich, A., and Schlessinger, J. (1990). Signal transduction by receptors with tyrosine kinase activity. Cell *61*, 203–212.

Vande Woude, G.F., Jeffers, M., Cortner, J., Alvord, G., Tsarfaty, I., and Resau, J. (1997). Met-HGF/SF: tumorigenesis, invasion and metastasis. Ciba Found Symp. *212*, 119–130.

Watabe, M., Matsumoto, K., Nakamura, T., and Takeichi, M. (1993). Effect of hepatocyte growth factor on cadherin-mediated cell-cell adhesion. Cell Struct. Funct. *18*, 117–124.

Weidner, K.M., Cesare, S.D., Sachs, M., Brinkmann, V., Behrens, J., and Birchmeier, W. (1996). Interaction between Gab 1 and the c-met receptor tyrosine kinase is responsible for epithelial morphogenesis. Nature *384*, 173–176.

Yang, Y., Spitzer, E., Meyer, D., Sachs, M., Niemann, C., Hartmann, G., Weidner, K.M., Birchmeier, C., and Birchmeier, W. (1995). Sequential requirement of HGF and neuregulin in the morphogenesis and differentiation of the mammary gland. J. Cell Biol. *131*, 215–226.

Yarden, Y., and Schlessinger, J. (1987). Epidermal growth factor induces rapid, reversible aggregation of purified epidermal growth factor receptor. Biochemistry *26*, 1443–1445.